

The Equation of State of Dense Matter: from Nuclear Collisions to Neutron Stars

G. F. Burgio

Istituto Nazionale di Fisica Nucleare, Sez. di Catania, Via S. Sofia 64, 95123
Catania, Italy

E-mail: fiorella.burgio@ct.infn.it

Abstract. The Equation of State (EoS) of dense matter represents a central issue in the study of compact astrophysical objects and heavy ion reactions at intermediate and relativistic energies. We have derived a nuclear EoS with nucleons and hyperons within the Brueckner-Hartree-Fock approach, and joined it with quark matter EoS. For that, we have employed the MIT bag model, as well as the Nambu–Jona-Lasinio (NJL) and the Color Dielectric (CD) models, and found that the NS maximum masses are not larger than 1.7 solar masses. A comparison with available data supports the idea that dense matter EoS should be soft at low density and quite stiff at high density.

1. Introduction

In the last few years, the study of the equation of state of nuclear matter has stimulated an intense theoretical activity. The interest for the nuclear EoS lies, to a large extent, in the study of compact objects, i.e., supernovae and neutron stars. In particular, the structure of a neutron star is very sensitive to the compressibility and the symmetry energy. For that, several phenomenological and microscopic models of the EoS have been developed. The former models include nonrelativistic mean field theory based on Skyrme interactions [1] and relativistic mean field theory based on meson-exchange interactions (Walecka model) [2]. The latter ones include nonrelativistic Brueckner-Hartree-Fock (BHF) theory [3] and its relativistic counterpart, the Dirac-Brueckner (DB) theory [4, 5], and the nonrelativistic variational approach also corrected by relativistic effects [6]. In these approaches the parameters of the interaction are fixed by the experimental nucleon-nucleon (NN) and/or nucleon-meson scattering data.

One of the most advanced microscopic approaches to the EoS of nuclear matter is the Brueckner theory. In the recent years, it has made a rapid progress in several aspects: (i) The convergence of the Brueckner-Bethe-Goldstone (BBG) expansion has been firmly established [7]. (ii) The addition of three-body forces (TBF) permitted to the agreement with the empirical saturation properties [8, 9]. (iii) The extension of the BHF approach has to the description of nuclear matter containing also hyperons [10], thus leading to a more realistic modeling of neutron stars [11, 12].

In the present paper we review these issues and present our results for neutron star structure based on the resulting EoS of dense hadronic matter, also supplemented by an eventual transition to quark matter at high density. A comparison with available experimental data from heavy ion collisions and neutron stars' observations will be discussed.

2. The Equation of State from the BBG approach

The Brueckner–Bethe–Goldstone (BBG) theory [3] is based on a linked cluster expansion of the energy per nucleon of nuclear matter. The basic ingredient in this many–body approach is the Brueckner reaction matrix G , which is the solution of the Bethe–Goldstone equation

$$G(\rho; \omega) = v + v \sum_{k_a k_b} \frac{|k_a k_b\rangle Q \langle k_a k_b|}{\omega - e(k_a) - e(k_b)} G(\rho; \omega), \quad (1)$$

where v is the bare nucleon-nucleon (NN) interaction, ρ is the nucleon number density, ω is the starting energy, and $|k_a k_b\rangle Q \langle k_a k_b|$ is the Pauli operator. $e(k) = e(k; \rho) = \frac{\hbar^2}{2m} k^2 + U(k; \rho)$ is the single particle energy, and the Brueckner–Hartree–Fock (BHF) approximation for the single particle potential $U(k; \rho)$ reads $U(k; \rho) = \sum_{k' \leq k_F} \langle k k' | G(\rho; e(k) + e(k')) | k k' \rangle_a$ (the subscript “ a ” indicates antisymmetrization of the matrix element). In the BHF approximation the energy per nucleon is

$$\frac{E}{A} = \frac{3}{5} \frac{\hbar^2}{2m} k_F^2 + D_{\text{BHF}}, \quad D_{\text{BHF}}(n) = \frac{1}{2A} \sum_{k, k' \leq k_F} \langle k k' | G(\rho; e(k) + e(k')) | k k' \rangle_a \quad (2)$$

In this scheme, the only input quantity we need is the bare NN interaction v in the Bethe–Goldstone equation (1). In this sense the BBG approach can be considered as a microscopic approach. However, it is well known that two-body forces are not able to explain some nuclear properties (e.g., binding energy of light nuclei, and saturation point of nuclear matter), and three-body forces (TBF) have to be introduced. In the framework of the Brueckner theory, a rigorous treatment of TBF would require the solution of the Bethe–Faddeev equation, describing the dynamics of three bodies embedded in the nuclear matter. In practice a much simpler approach is employed, namely the TBF is reduced to an effective, density-dependent, two-body force by averaging over the third nucleon in the medium, taking account of the nucleon-nucleon correlations. This effective two-body force is added to the bare two-body force and recalculated at each step of the iterative procedure.

Both phenomenological and microscopic TBF have been used in the BHF approach. The phenomenological TBF is widely used in the literature, in particular the Urbana IX TBF [13] for variational calculations of finite nuclei and nuclear matter [6], and contains a two-pion exchange potential, which is attractive at low density, and a phenomenological repulsive term, more effective at high density. The microscopic TBF is based on meson-exchange mechanisms accompanied by the excitation of nucleonic

resonances [8, 9], and produces a remarkable improvement of the saturation properties of nuclear matter [9].

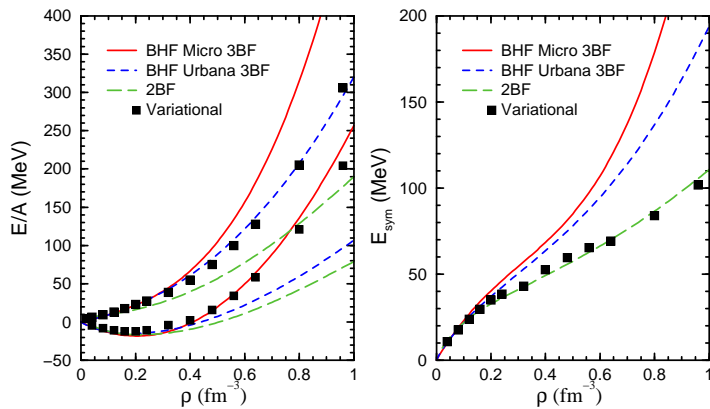


Figure 1. In the left panel, symmetric matter (lower curves) and pure neutron matter (upper curves) EoS, calculated within the BBG approach, are shown. Variational many-body calculations are also displayed (full squares). The symmetry energy is shown in the right panel.

Let us now compare the EoS predicted by the BHF approximation with the same two-body force (Argonne v_{18} [14]) and different TBF [15]. In the left panel of Fig. 1 we display the EoS both for symmetric matter (lower curves) and pure neutron matter (upper curves). We show results obtained for several cases, i.e., i) only two-body forces are included (long dashed lines), ii) TBF treated within the phenomenological Urbana IX model (dashed lines), and the microscopic meson-exchange approach (solid lines). For completeness, we also show results obtained with variational calculations (full squares) [6]. We notice that the EoS for symmetric matter with TBF reproduces the correct nuclear matter saturation point in all approaches. Moreover, up to a density of $\rho \approx 0.4 \text{ fm}^{-3}$ the BHF EoS calculated with TBF are in fair agreement with the variational calculations, whereas at higher density the microscopic TBF turns out to be the most repulsive. In all cases, the incompressibility at saturation is compatible with the values extracted from phenomenology, i.e., $K \approx 210 \text{ MeV}$. In the right panel of Fig. 1 we display the symmetry energy as a function of the nucleon density ρ . Within the BHF approach, the symmetry energy has been calculated within the so-called “parabolic approximation” for the binding energy of nuclear matter with arbitrary proton fraction [16]. We observe results in agreement with the characteristics of the EoS shown in the left panel, namely, the stiffest EoS yields larger symmetry energies compared to the ones obtained with the Urbana phenomenological TBF and the variational calculations. This leads to a different proton fraction in beta-stable nuclear matter. We notice that the symmetry energy calculated (with or without TBF) at the saturation point yields a value $E_{\text{sym}} \approx 30 \text{ MeV}$, compatible with nuclear phenomenology.

In the last few years it became popular to compare the various microscopic and phenomenological EoS with the allowed region in the pressure–density plane, as

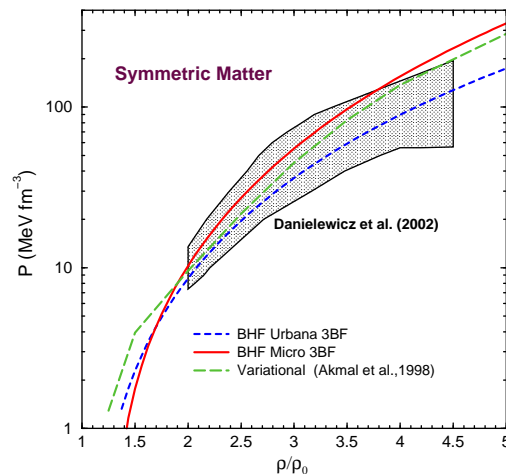


Figure 2. Different EoS are compared with the phenomenological constraint extracted by Danielewicz et al. [17] (shaded area). Solid (dashed) line: BHF EoS with microscopic (phenomenological) TBF. Long dashed line : variational EoS.

determined by Danielewicz et al. [17]. In that paper the authors consider both the in-plane transverse flow and the elliptic flow measured in different experiments on $Au + Au$ collisions at energies between 0.2 and 10 GeV/A. From the data, Danielewicz et al. could estimate the pressure for symmetric matter. In Fig. 2 the set of microscopic EoS discussed is displayed along with the allowed pressure region (shaded area). Both the EoS derived from BHF with Urbana IX TBF and the variational one are in agreement with the phenomenological analysis, while the BHF EoS with microscopic TBF turns out to be only marginally compatible, since at higher density it becomes too stiff and definitely falls outside the allowed region. Additional analyses of flow data, as reported by the FOPI Collaboration [18], and subthreshold K^+ production [19] confirm a soft equation of state in the same density range (see C. Fuchs contribution to this conference).

3. Hyperons in nuclear matter

While at moderate densities $\rho \approx \rho_0$ the matter inside a neutron star consists only of nucleons and leptons, at higher densities several other species of particles may appear due to the fast rise of the baryon chemical potentials with density. Among these new particles are strange baryons, namely, the Λ , Σ , and Ξ hyperons. Due to its negative charge, the Σ^- hyperon is the first strange baryon expected to appear with increasing density in the reaction $n + n \rightarrow p + \Sigma^-$, in spite of its substantially larger mass compared to the neutral Λ hyperon ($M_{\Sigma^-} = 1197$ MeV, $M_{\Lambda} = 1116$ MeV). Other species might appear in stellar matter, like Δ isobars along with pion and kaon condensates.

We have generalized the study of the nuclear EoS with the inclusion of the Σ^- and Λ hyperons in the BHF many-body approach. To this purpose, one requires in principle nucleon-hyperon (NH) and hyperon-hyperon (HH) potentials. In our work we use the Nijmegen soft-core NH potential [20], that is well adapted to the existing experimental

NH scattering data. Unfortunately, up to date no HH scattering data exist and therefore no reliable HH potentials are available. Hence we neglected HH potentials in our BHF calculations [11]. Nevertheless, the importance of HH potentials should be minor as long as the hyperonic partial densities remain limited.

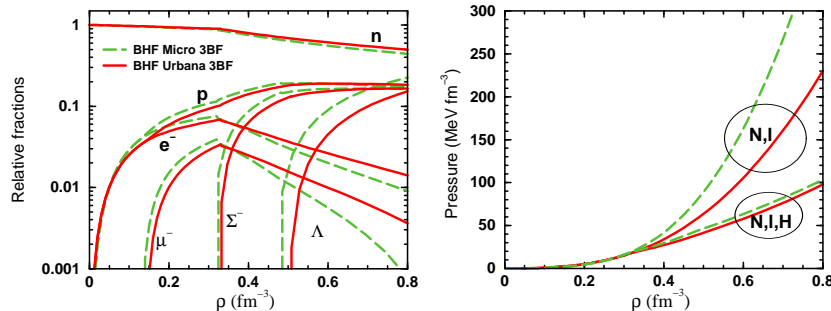


Figure 3. The particle concentrations (left panel) are shown as function of the baryon density. Long dashed curves are calculations performed with the microscopic TBF, whereas solid lines represent the Urbana TBF calculations. In the right panel the corresponding EoS are shown.

In Fig. 3 (left panel) we show the chemical composition of the resulting beta-stable and asymmetric nuclear matter containing hyperons. We observe rather low hyperon onset densities of about 2-3 times normal nuclear matter density for the appearance of the Σ^- and Λ hyperons, almost independently on the adopted TBF. Moreover, an almost equal percentage of nucleons and hyperons are present in the stellar core at high densities. A strong deleptonization of matter takes place, and this can have far reaching consequences for the onset of kaon condensation [21]. The resulting EoS is displayed in the right panel of Fig. 3. The upper curves show the EoS when stellar matter is composed only of nucleons and leptons, whereas the lower curves show calculations with nucleons and hyperons. We notice that the inclusion of hyperons produces a much softer EoS, no matter the TBF adopted in the nucleonic sector. These remarkable results are due to the inclusion of hyperons as additional degrees of freedom, and we do not expect substantial changes when introducing refinements of the theoretical framework, such as hyperon-hyperon potentials, hyperonic TBF, relativistic corrections, etc.

The consequences for the structure of the neutron stars are illustrated in Fig. 4, where we display the resulting neutron star mass-radius curves, obtained solving the Tolman-Oppenheimer-Volkoff equations [22]. We notice that the BHF EoS calculated with the microscopic TBF produces the largest gravitational masses, with the maximum mass of the order of $2.3 M_\odot$, whereas the phenomenological TBF yields a maximum mass of about $1.9 M_\odot$. In the latter case, neutron stars are characterized by smaller radii and larger central densities, i.e., the Urbana TBF produce more compact stellar objects. One should notice that, although different TBF still yield quite different maximum masses, the presence of hyperons equalizes the results, leading now to a maximum mass of less than 1.3 solar masses for all the nuclear TBF. This result is in contradiction with the measured value of the Hulse-Taylor pulsar mass, PSR1913+16, which amounts to 1.44

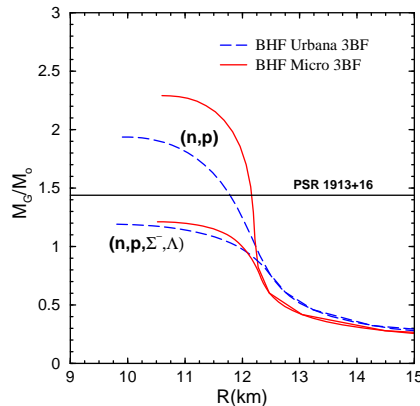


Figure 4. The mass-radius relation is plotted for EoS without hyperons (upper curves), and with hyperons (lower curves). See text for details.

M_{\odot} . The only remaining possibility in order to reach significantly larger maximum masses appears to be the transition to another phase of dense (quark) matter inside the star. This is indeed a reasonable assumption, since already geometrically the concept of distinguishable baryons breaks down at the densities encountered in the interior of a neutron star. This will be discussed in the following.

4. Quark matter

The results obtained with a purely hadronic EoS call for an estimate of the effects due to the hypothetical presence of quark matter in the interior of the neutron star. Unfortunately, the current theoretical description of quark matter is burdened with large uncertainties, seriously limiting the predictive power of any theoretical approach at high baryonic density. For the time being we can therefore only resort to phenomenological models for the quark matter EoS, and try to constrain them as well as possible by the few experimental information on high-density baryonic matter.

One of these constraints is the phenomenological observation that in heavy ion collisions at intermediate energies ($10 \text{ MeV}/A \lesssim E/A \lesssim 200 \text{ MeV}/A$) no evidence for a transition to a quark-gluon plasma has been found up to about $3\rho_0$. We have taken this constraint in due consideration, and used an extended MIT bag model [23] (including the possibility of a density dependent bag “constant”) and the color dielectric model [24], both compatible with this condition [25]. For completeness, we have also used the Nambu–Jona-Lasinio model [26].

In order to study the hadron-quark phase transition in neutron stars, we have performed the Maxwell construction, so demanding a sharp phase transition. We have found that the phase transition in the extended MIT bag model takes place at a large baryon density, $\rho \approx 0.6 \text{ fm}^{-3}$, and at larger baryon density in the NJL model [26]. On the contrary, the transition density in the CD model is $\rho \approx 0.05 \text{ fm}^{-3}$. This implies a large difference in the structure of hybrid stars. In fact, whereas stars built with the CD model have at most a mixed phase at low density and a pure quark core at higher

density, the ones obtained with the MIT bag model contain a hadronic phase, followed by a mixed phase and a pure quark interior. The scenario is again different within the Nambu-Jona-Lasinio model, where at most a mixed phase is present, but no pure quark phase. The final result for the structure of hybrid neutron stars is shown in Fig. 5,

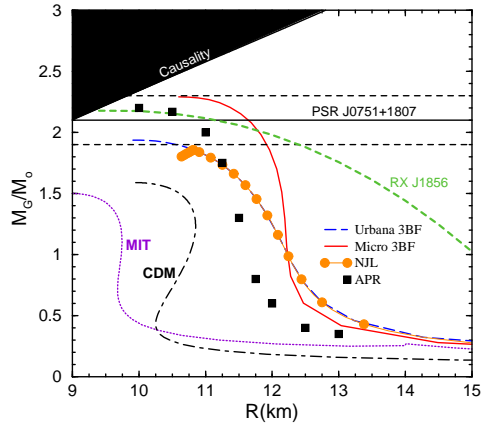


Figure 5. The mass-radius relation is shown for the several cases discussed in the text, along with some observational constraints.

displaying the mass-radius relation. It is evident that the most striking effect of the inclusion of quark matter is the increase of the maximum mass with respect to the case with hyperons, now reaching about $1.5 M_\odot$. At the same time, the typical neutron star radius is reduced by about 3 km to typically 9 km. Hybrid neutron stars are thus more compact than purely hadronic ones and their central energy density is larger. In Fig. 5 we also display some observational constraints. The first one demands that any reliable EoS should be able to reproduce the recently reported high pulsar mass of $2.1 \pm 0.2 M_\odot$ for PSR J0751+1807 [27]. Extending this value even to 2σ confidence level ($^{+0.4}_{-0.5} M_\odot$) means that masses of at least $1.6 M_\odot$ have to be allowed. The other constraint comes from a recent analysis of the thermal radiation of the isolated pulsar RX J1856 which determines a lower bound for its mass-radius relation that implies a rather stiff EoS [28]. Both constraints indicate that the EoS should be rather stiff at high density. Moreover, if quark matter is present in the neutron stars' interiors, this would require additional repulsive contributions in the quark matter EoS.

5. Conclusions

In this paper we reported the theoretical description of nuclear matter in the BHF approach, with the application to neutron star structure calculation. We pointed out the important role of TBF at high density, which is, however, strongly compensated by the inclusion of hyperons. The resulting hadronic neutron star configurations have maximum masses of less than $1.4 M_\odot$, and the presence of quark matter inside the star is required in order to reach larger values.

Concerning the treatment of quark matter, we have joined the corresponding EoS with the hadronic one, and reached maximum masses of about $1.7 M_{\odot}$. The value of the maximum mass of neutron stars obtained according to our analysis appears rather robust with respect to the uncertainties of the nuclear and the quark matter EoS. Therefore, the experimental observation of a very heavy ($M \gtrsim 1.7 M_{\odot}$) neutron star would suggest that serious problems are present for the current theoretical modelling of the high-density phase of nuclear matter. In any case, one can expect a well defined hint on the high-density nuclear matter EoS.

References

- [1] Bonche P, Chabanat E, Haensel P, Meyer J, and Schaeffer R 1998, Nucl. Phys. **A635** 231.
- [2] Serot B D, and Walecka J D 1986, Adv. Nucl. Phys. **16** 1.
- [3] Baldo M, in *Nuclear Methods and the Nuclear Equation of State*, International Review of Nuclear Physics, Vol.8, (World Scientific, Singapore, 1999).
- [4] Machleidt R 1989, Adv. Nucl. Phys. **19** 189; Li G Q, Machleidt R, and Brockmann R 1992, Phys. Rev. **C45** 2782; Krastev P G, and Sammarruca F 2006, Phys. Rev. **C74** 025808.
- [5] Gross-Boelting T, Fuchs C, Faessler A 1999, Nucl. Phys.**A 648** 105; van Dalen E, Fuchs C, Faessler A 2004, Nucl. Phys.**A 744** 227; 2005, Phys. Rev. Lett. **95** 022302; 2007, Eur. Phys. J. **A 31** 29.
- [6] Akmal A, Pandharipande V R , and Ravenhall D G 1998, Phys. Rev. **C58** 1804.
- [7] Day B D 1981, Phys. Rev. **C24** 1203; Song H Q, Baldo M, Giansiracusa G, and Lombardo U 1998, Phys. Rev. Lett. **81** 1584; Baldo M, Fiasconaro A, Song H Q, Giansiracusa G, and Lombardo U 2002, Phys. Rev. **C65** 017303.
- [8] Grangé P, Lejeune A, Martzolff M, and Mathiot J-F 1989, Phys. Rev. **C40** 1040.
- [9] Zuo W, Lejeune A, Lombardo U, and Mathiot J-F 2002, Prog. Theor. Phys. Suppl. **146** 478.
- [10] Schulze H-J, Baldo M, Lombardo U, Cugnon J, and Lejeune A 1998, Phys. Rev. **C57** 704.
- [11] Baldo M, Burgio G F, and Schulze H-J 2000, Phys. Rev. **C61** 055801.
- [12] Schulze H-J, Polls A, Ramos A, and Vidaña I 2006, Phys. Rev. **C73** 058801.
- [13] Carlson J, Morales J, Pandharipande V R, and Ravenhall D G 2003, Phys. Rev. **C68** 025802.
- [14] Wiringa R B, Stoks V G J , and Schiavilla R 1995, Phys. Rev. **C51** 38.
- [15] Zhou X R, Burgio G F , Lombardo U, Schulze H-J and Zuo W 2004, Phys. Rev. **C 69** 018801.
- [16] Bombaci I, and Lombardo U 1991, Phys. Rev. **C44** 1892.
- [17] Danielewicz P, Lacey R, and Lynch W G 2002, Science **298** 1592.
- [18] Stoicea G et al. [FOPI Collaboration] 2004, Phys. Rev. Lett. **92** 072303.
- [19] Sturm C et al. [KaoS Collaboration] 2001, Phys. Rev. Lett. **86** 39; Schmah A et al. [KaoS Collaboration] 2005, Phys. Rev. **C71** 064907.
- [20] Maessen P M M, Rijken Th A, and de Swart J J 1989, Phys. Rev. **C40** 2226.
- [21] Li A, Burgio G F, Lombardo U, and Zuo W 2006, Phys. Rev. **C74** 055801.
- [22] Shapiro S and Teukolsky S A, *Black Holes, White Dwarfs, and Neutron Stars*, (John Wiley & Sons, New York, 1983)
- [23] Chodos A, Jaffe R L , Johnson K, Thorn C B, and Weisskopf V F 1974, Phys. Rev. **D9** 3471.
- [24] Pirner H J, Chanfray G, and Nachtmann O 1984, Phys. Lett. **B147** 249; Drago A, Tambini U, and Hjorth-Jensen M 1996, Phys. Lett. **B380** 13.
- [25] Maieron C, Baldo M, Burgio G F, and Schulze H-J 2004, Phys. Rev. **D70** 043010.
- [26] Baldo M, Buballa M, Burgio G F, Neumann F, Oertel M, and Schulze H-J 2003, Phys. Lett. **B562** 153.
- [27] Nice D J, Splaver E M, Stairs I H , Löhmer O, Jessner A, Kramer M, and Cordes J M 2005, Astrophys. J. **634** 1242.
- [28] Trümper J E, Burwitz V, Haberl F, and Zavlin V E 2004, Nucl. Phys. Proc. Suppl. **132** 560.